Journal of Inflammation Research

Dovepress
Taylor & Francis Group

Open Access Full Text Article

ORIGINAL RESEARCH

Mechanistic Insights Into the Modulation of Gut Microbiota and ERK Signaling by Morusin in Juvenile Rats with Post-Infectious Cough

Jing Luo[1], Dan Zhang[1], Miaomiao Zhang[1], Yiqiang Chen[1], Yi Ding[2]

[1]Department of Chinese Medicine, Shenzhen Qianhai Shekou Free Trade Zone Hospital, Shenzhen, Guangzhou, People's Republic of China; [2]Department of Physical Medicine and Rehabilitation, Changsha Social Work College, Changsha, Hunan, People's Republic of China

Correspondence: Yi Ding, Department of Physical medicine and rehabilitation, Changsha Social Work College, Changsha, Hunan, People's Republic of China, 410004, Email zyk20240403@163.com

Journal of Inflammation Research downloaded from https://www.dovepress.com/
For personal use only.

Background: Post-infectious cough (PIC) is a leading cause of chronic cough in children, often persisting after respiratory infections and significantly impairing quality of life. Current therapies, such as montelukast sodium (MAS), offer only partial symptom relief and do not target the underlying inflammatory and microbiota-driven mechanisms. Emerging evidence suggests that the lung–gut axis, ERK pathway activation, and cytokine–microbiota interactions are central to PIC pathogenesis. Morusin, a prenylated flavonoid from Morus alba, possesses anti-inflammatory and barrier-protective activities and may uniquely modulate both ERK signaling and gut microbiota, offering mechanistic advantages over conventional treatments.

Methods: A juvenile rat model of PIC was induced by smoke exposure, lipopolysaccharide nasal instillation, and capsaicin atomization. Rats were assigned to control, model, morusin, or MAS groups. Physiological outcomes, histology, and immunostaining were assessed, including body weight, airway resistance, goblet cells, cytokines (IL-4, IL-6, IL-10), and phosphorylated ERK1/2 (p-ERK1/2) in lung and colon tissues. Gut microbiota was profiled via 16S rRNA sequencing, with correlation analyses linking microbial changes to cytokine and signaling profiles.

Results: Morusin improved systemic parameters (body weight, salivary flow, skin hydration), reduced airway hyperreactivity, and normalized anxiety-like behaviors, effects not observed with MAS. Both morusin and MAS reduced lung goblet cell hyperplasia and inflammatory cytokines, but only morusin suppressed p-ERK1/2 in both lung and colon tissues and reshaped the gut microbiota. Morusin enriched beneficial genera (Lactobacillus, Akkermansia) and reduced pro-inflammatory taxa (Ruminococcus, Lachnospiraceae_NK4A136_group). Correlation analyses confirmed strong links between microbial shifts, cytokine balance, and ERK modulation.

Conclusion: Morusin alleviates PIC through systemic, mucosal, and behavioral improvements, combined with unique modulation of gut microbiota and ERK signaling across the lung–gut axis. These findings highlight morusin's novel mechanistic advantage over MAS and support its potential as a translational therapy for pediatric PIC.

Keywords: morusin, post-infectious cough, air way inflammation, p-ERK, gut microbiota

Introduction

Post-infectious cough (PIC), a frequently occurring chronic cough in children, is believed to develop following respiratory tract pathogen infections that impair respiratory barrier function.[1] This damage triggers inflammation and heightened airway sensitivity, prolonging the cough.[2] Treatment mainly involves antitussive, anti-inflammatory and expectorant medications, tailored to the underlying cause.[2] However, specific drugs targeting PIC in children are currently lacking.

Morusin is a prenylated flavonoid isolated from the root bark of Morus alba that has demonstrated potent anti-inflammatory and barrier-protective activities.[3–5] In vitro, morusin markedly suppresses IL-1β-induced upregulation of pro-inflammatory mediators (TNF-α, IL-6, iNOS, COX-2), inhibits extracellular matrix-degrading enzymes (ADAMTS5,

Received: 28 June 2025
Accepted: 8 October 2025
Published: 19 November 2025

© 2025 Luo et al. This work is published and licensed by Dove Medical Press Limited. The full terms of this license are available at https://www.dovepress.com/terms.php and incorporate the Creative Commons Attribution – Non Commercial (unported, v4.0) License (http://creativecommons.org/licenses/by-nc/4.0/). By accessing the work you hereby accept the Terms. Non-commercial uses of the work are permitted without any further permission from Dove Medical Press Limited, provided the work is properly attributed. For permission for commercial use of this work, please see paragraphs 4.2 and 5 of our Terms (https://www.dovepress.com/terms.php).

MMPs), and prevents NF-κB p65 phosphorylation and IκBα degradation in chondrocytes, effects that translate into cartilage protection in an osteoarthritis model in vivo.[6] In epithelial cells challenged with LPS, morusin downregulates EGFR-mediated AKT and NF-κB signaling, reduces inflammatory cytokine expression, and enhances barrier integrity in a concentration-dependent manner.[7] Beyond these settings, morusin exhibits broad antioxidant and immunomodulatory properties, suppressing STAT1 and NF-κB activation in keratinocytes, inhibiting mast cell degranulation, and attenuating oxidative stress and apoptosis across multiple cell types, highlighting its potential as a multitarget therapeutic agent.[3]

The gut microbiota significantly influences immune system development and the maintenance of homeostasis. Recent research has linked respiratory/gastrointestinal tract microbiota shifts in altered immune responses and the progression of lung diseases.[8] Some studies suggest a connection between gut microbiota and PIC pathogenesis.[9,10] Accumulating evidence also suggests that morusin can beneficially modulate the gut microbiota. Exosome-like nanoparticles derived from mulberry bark, rich in morusin, activate the AhR/COPS8 pathway in intestinal epithelial cells, inducing antimicrobial peptides and protecting against DSS-induced colitis.[11] In a type 2 diabetic mouse model, mulberry leaf water extract, which contains morusin, reshapes gut microbial communities by reducing lipopolysaccharide-producing genera and restoring barrier and endocannabinoid system homeostasis.[12] Moreover, mulberry fruit administration increases short-chain fatty acid–producing bacteria (eg, Lactobacillus, Bifidobacterium), elevates fecal SCFAs, and alleviates constipation in mice.[13] Together, these studies imply that morusin may exert PIC-ameliorating effects not only through direct anti-inflammatory signaling but also by fostering a beneficial gut microbiota. However, the specific pathways through which morusin links gut microbiota modulation to airway inflammation, particularly via immune signaling and the lung–gut axis, remain poorly defined.

Extracellular signal-regulated kinases 1 and 2 (ERK1/2) are critical components of the MAPK signaling pathway, playing a significant role in mediating inflammatory responses and airway sensitivity,[14] both of which are key features of PIC.[15] Inflammation driven by ERK1/2 activation can lead to heightened airway reactivity and prolonged cough.[16] Additionally, ERK1/2 signaling is involved in the lung-gut axis, where alterations in gut microbiota can influence immune responses and respiratory health.[17,18] Notably, morusin has been shown to bidirectionally modulate ERK1/2. In human lung carcinoma cells, morusin activates ERK (alongside JNK and PI3K/Akt), driving ROS-dependent apoptosis and autophagy,[19] whereas in nasopharyngeal carcinoma it suppresses ERK1/2 phosphorylation to downregulate MMP-2 expression and inhibit cell invasion.[20] Given its capacity to both inhibit and fine-tune ERK1/2 activity depending on context, morusin represents a promising therapeutic for PIC by potentially reducing airway inflammation and normalizing airway function through targeted ERK1/2 modulation.

Therefore, although morusin has demonstrated strong anti-inflammatory and microbiota-regulating activities, the mechanistic links between these effects, particularly its regulation of ERK signaling within the lung–gut axis, have not been fully elucidated. We hypothesized that morusin could alleviate PIC by modulating gut microbiota and suppressing ERK signaling, thereby reducing airway inflammation and hyperreactivity. To test this, we evaluated pathological changes, immune responses, and microbial alterations in a PIC rat model treated with morusin.

Materials and Methods

Animals

Forty young male Sprague-Dawley (SD) rats, SPF grade, weighing between 60 to 80 g and aged 3 to 4 weeks, were procured from Hunan Slike Jingda Co., Ltd. [Animal Health Certificate: SCXK (Xiang) 2019–0004, Quality Certificate Number: No.430727211102546963]. The housing temperature ranged from 20.0 to 27.5°C, with 45.0% to 68.0% relative humidity. The rats followed a 12-hour light-dark cycle and had ad libitum access to water. Rat feed, supplied by Hunan Jiatai Experimental Animal Co., Ltd., had license number SCXK (Xiang) 2020–0006 and feed quality certificate number No.2021051110099. All the animal experiments were approved by the Animal Ethics Committee of Shenzhen Qianhai Shekou Free Trade Zone Hospital (No.20210110). The experiments were conducted in strict compliance with the National Laboratory Animal Welfare Standards: Laboratory Animal—Guideline for Ethical Review of Animal Welfare (GB/T35892–2018).

Rat PIC Model and Drug Treatments

Animals were subject to acclimatization for 7 days, after which ten rats were randomly assigned as the control group. Remaining animals were subjected to fumigation, nasal instillation of lipopolysaccharide (LPS: at a concentration of 0.4 mg/mL at a volume of 1 μL/g once daily), and N-Vanillylnonanamide (V10723721) atomization to induce PIC. Fumigation was conducted on 1st day to induce airway hyperresponsiveness, utilizing a homemade smoke box containing a mixture of sawdust and cigarettes. This exposure occurred twice daily for 30 minutes each time over ten consecutive days. Meanwhile, airway inflammation was induced by nasal LPS treatment on 11^{th}, 14^{th} and 17^{th} day, while cough was elicited by N-Vanillylnonanamide atomization on 12^{th}, 14^{th}, 15^{th}, 16^{th} and 16^{th} day.

On the 18th day, a provocative cough was challenged with N-Vanillylnonanamide was performed to confirm successful model induction. Criteria for successful modeling included observable coughing, foot and neck extension, accelerated breathing, abdominal muscle contraction, and a cough frequency exceeding 10 times within 3 minutes. Based on our preliminary experiments (n = 3), we hypothesized a reduction of 15% (mean difference) in airway resistance after XBZY treatment comparing to model group with an alpha level of 5% and a power of 80% and calculated that a sample size of 10 would be required for this study. Thus, we used n = 10 in our work. Animals meeting these criteria were randomly assigned to the model group (n=10), morusin group (n=10), and MAS group (n=10). Rats in model and groups received oral gavage of saline, while those in the morusin group received morusin (40 mg/kg: Sigma-Aldrich) treatment,[6,21] and those in the MAS group received montelukast sodium solution (1 mg/kg), once daily from 13^{th} to 19^{th} day.

Twenty-four hours after last intervention, rats were euthanized under anesthesia, and tissues from the lung and colon were collected for further analysis. Fecal samples were also collected and stored at −80°C for subsequent analysis. Tissue samples were processed for histological analysis after fixation and embedding in paraffin. Group allocation was carried out by a designated researcher who was aware of the assignments to ensure accurate dosing and intervention. During the experiment, treatment administrators were necessarily unblinded because of the distinct preparation of study drugs. All outcome assessments were performed by investigators blinded to group allocation. Data entry and statistical analyses were conducted by an independent researcher who remained blinded to group assignments until completion of the analysis.

Airway Resistance Testing

Following intraperitoneal injection of pentobarbitone (40 mg/kg) for rat anesthesia, the animals were positioned supine and securely immobilized. A surgical incision was made over the neck to expose the trachea, which was then dissected in a T-shape. Subsequently, a tracheal tube was carefully inserted, and the rat was placed within a closed-body plethysmograph. Mechanical ventilation was initiated using a ventilator set to a frequency of 75 breaths/min and an 8 mL/kg tidal volume. Baseline airway resistance values were recorded once stabilization was achieved. Aerosolized acetylcholine solutions at various concentrations (6.25–50 mg/mL, with saline as the 0 dose) were administered, and changes in airway resistance relative to baseline were monitored and recorded.

Saliva Flow Rate

Using tweezers, place filter paper in the rat's mouth, allowing it to remain on the tongue surface for 5 seconds before removing it. Weigh the filter paper using an electronic balance. The salivary flow rate (mg/s) is calculated as (wet weight of filter paper - dry weight of filter paper) / 5 s. This process is repeated every hour, with three measurements taken each time, and the average is calculated.

Rectal Temperature

Using an infrared thermometer, measure the rectal temperature of rats in each group. Position the thermometer probe 1–2 cm from the center of the detection site.

Open Field Test

The open-field test chamber is divided into 16 squares, each measuring 20 cm × 20 cm, at the bottom. Rats are gently placed in the central area of the chamber, and EthoVision 3.0 behavior analysis software is used to analyze and evaluate the rats' activity over 5 minutes. This includes the number of central zone crossings, time spent in the central zone, total distance moved, and velocity. The surrounding environment is kept quiet during the experiment. After each rat's experiment, the chamber is cleaned of feces, and the equipment is wiped with 75% ethanol to eliminate odors that may affect the rats.

Water Content in the Skin

Using a shaver, remove the hair from an area on the rat's back approximately 1 cm × 1 cm in size to fully expose the skin. This area is designated for measuring the moisture content of the back skin. Skin moisture content is also measured at the paw pads of the limbs. A skin moisture and oil tester is used to assess the moisture content of both the rat's back and limbs.

Periodic Acid-Schiff (PAS) Staining of Lung and Colon Samples

Paraffin-embedded tissues were sliced into 5-μm sections for PAS staining, aimed at assessing the histopathological profile and mucus production. These tissue sections were subsequently examined under a light microscope. Using Image-Pro Plus 7.0 image analysis software, five random high-power microscope images featuring bronchi were selected from each lung tissue section. The area occupied by intact goblet cells within the bronchial mucosal epithelium was quantified as a percentage of the total epithelial area. For each colon tissue section, three random fields were selected, and the total number of goblet cells was counted. This count was then divided by the number of villi in each field to determine the goblet cell density within the rat's colonic mucosal epithelium.

Immunostaining Analysis

Paraffin-embedded sections were cut into 5-μm slices and permeabilized with 1% Triton X-100 in phosphate-buffered saline (PBS) for 30 minutes. They were then subjected to antigen retrieval by boiling in 100 mM sodium citrate (pH 6.0) three times, each for 6 minutes. Following this, the sections were treated with 3% hydrogen peroxide for 30 minutes and then blocked with 5% bovine serum albumin at room temperature for 1 hour.

Next, sections were incubated overnight at 4°C with primary rabbit antibodies, including IL-4, IL-6, IL-10, and phospho-ERK1/2 (p-ERK1/2) (diluted at 1:100; ab178876, Abcam, USA), while normal IgG was utilized for proper control. Subsequently, sections were probed by rabbit anti-goat biotin-SP-conjugated antibody (Protein Tech Group Inc.) at room temperature for 1hour. Stained proteins were detected by 3,3'-diaminobenzidine chromogen.

Extraction of Intestinal Microbiota DNA and Analysis of Sequencing Data

The DNA was extracted from fecal samples, and the V3-V4 variable region of the 16S rRNA gene was PCR amplified using forward primer 338F (5'- AC TCC TAC GGG AGG CAG CAG −3') and reverse primer 806R (5'-GGA CTA CHV GGG TWT CTA AT-3') carrying Barcode sequences. After purification, PCR products were library constructed using the NEXTFLEX Rapid DNA-Seq Kit. Quality control of the paired-end raw sequencing reads was carried out by fastp (https://github.com/OpenGene/fastp, version 0.19.6). FLASH software (http://www.cbcb.umd.edu/software/flash, version 1.2.11) was used for merging, and UPARSE software (http://drive5.com/uparse/, version 7.1) was utilized for operational taxonomic unit (OTU) clustering and chimaera removal at 97% similarity threshold.

OTUs were taxonomically annotated against Silva 16S rRNA gene database (v138) with a confidence threshold of 70%. Community composition was examined at various taxonomic levels. All data analysis was conducted on Meiji Biological Cloud Platform. Kruskal–Wallis rank-sum test was employed for differential analysis of intestinal microbiota among different rat groups. LEfSe (Linear discriminant analysis Effect Size) was utilized for multi-level species differential analysis to identify significantly differentially abundant taxa among groups, with an LDA threshold of 4, genus-level classification, and All-against-all (more strict) multi-group comparison. Spearman correlation analysis was used to explore relationship of environmental factors and microbial composition.

Statistical Analysis

Experimental results are expressed as mean ± standard deviation. Statistical analysis was conducted using SPSS 18.0 software (SPSS, Inc., Chicago, IL, USA). The normality of the data distribution was assessed using the Kolmogorov–Smirnov test. One-way ANOVA followed by Bonferroni's multiple comparison tests or Kruskal–Wallis *H*-test was employed for comparisons among multiple groups as appropriate. The correlation between bacterial abundance and environmental factors was assessed by Pearson's correlation analysis. A significance level of $P < 0.05$ was considered statistically significant.

Results

Actions of Morusin and MAS on Body Weight, Rectal Temperature and Saliva Flow Rate

Body weight and saliva flow rate were reduced, and rectal temperature was elevated in rats from the model group compared to the control group (Body weight: model group, 340.9±14.3 g versus control group, 394.7±16.4, P<0.01; saliva flow rate: mode group, 0.77±0.06 mg/s versus control group 1.29 ± 0.06 mg/s, P<0.01; rectal temperature: model group, 37.8±0.4 °C versus control group, 36.6±0.5 °C, P<0.01; n = 10; Figure 1). In the morusin group, body weight and saliva flow rate increased, and rectal temperature decreased compared to the model group (Body weight: morusin group, 360.2 ± 9.6 g versus model group, 340.9 ± 14.3 g, P<0.05; rectal temperature: morusin group, 37.3 ± 0.3 °C versus model group, 37.9 ± 0.4 °C, P<0.05; saliva flow rate: morusin group, 1.14 ± 0.09 mg/s versus model group, 0.77 ± 0.06 mg/s, P<0.01; n = 10; Figure 1). MAS treatment had no effect on body weight, saliva flow rate, or rectal temperature in the PIC model rats (Body weight: MAS group, 348.0 ± 9.6 g versus model group, 340.9 ± 14.3 g, P>0.05; rectal temperature: MAS group, 37.5 ± 0.3 °C versus model group, 37.9 ± 0.4 °C, P>0.05; saliva flow rate: MAS group, 0.79 ± 0.06 mg/s versus model group, 0.77 ± 0.06 mg/s, P>0.05; n = 10; Figure 1).

Effects of Morusin and MAS on the Water Content in the Rat Skin

The skin water content of the paw pads in the model group was reduced compared to the normal group ((Paw pad of left forelimb: model group, 29.2 ± 1.7 versus control group, 32.7 ± 2.5, P<0.05; paw pad of right forelimb: model group, 28.7 ± 2.5 versus control group, 32.8 ± 2.3, P<0.05; paw pad of left hindlimb: model group, 30.4 ± 1.3 versus control group, 32.4 ± 1.2, P<0.05; paw pad of right hindlimb: model group, 29.7 ± 1.1 versus control group, 32.8 ± 2.2, P<0.05; n = 10; Figure 2), with a decreasing trend in back skin water content that was not statistically significant (Back: model group, 24.0 ± 0.6 versus control group, 24.8 ± 1.1, P>0.05; n = 10; Figure 2). Compared to the model group, rats in the morusin treatment group showed a significant increase in skin water content in both the paw pads and the back (Paw pad of left forelimb: morusin group, 31.5 ± 1.3 versus model group, 29.2 ± 1.7, P<0.05; paw pad of right forelimb: morusin group, 32.0 ± 1.1 versus model group, 28.7 ± 2.5, P<0.05; paw pad of left hindlimb: morusin group, 32.6 ± 1.6 versus model group, 30.4 ± 1.3, P<0.05; paw pad of right hindlimb: morusin group, 32.1 ± 1.5 versus model group, 29.7 ± 1.1, P<0.05; back: morusin group, 25.0 ± 0.8 versus model group, 24.0 ± 0.6, P<0.05; n = 10; Figure 2). MAS had no effect on skin water content in the PIC model rats (Paw pad of left forelimb: MAS group, 30.2 ± 2.9 versus model group, 29.2 ± 1.7, P>0.05; paw pad of right forelimb: MAS group, 30.5 ± 2.7 versus model group, 28.7 ± 2.5, P>0.05; paw pad of left hindlimb: MAS group, 30.2 ± 2.2 versus model group, 30.4 ± 1.3, P>0.05; paw pad of right hindlimb: MAS group, 30.8 ± 2.4 versus model group, 29.7 ± 1.1, P>0.05; back: MAS group, 24.0 ± 0.6 versus model group, 24.0 ± 0.6, P>0.05; n = 10; Figure 2).

Open Field Test of the Rats with Different Treatments

The number of central zone crossings, time spent in the central zone, total distance moved, and velocity were significantly elevated in rats from the model group compared to the control group (Number of central zone crossings: model group, 14.2 ± 2.6 versus control group, 8.7 ± 1.4, P<0.01; time spent in the central zone: model group, 24.8 ± 2.3% versus control group, 12.3 ± 2.8%, P<0.01; total distance moved: model group, 55.0 ± 2.7 m versus control group, 38.2 ± 2.0 m, P<0.01; velocity: model group, 22.2 ± 3.7 mm/s versus control group, 15.6 ± 1.9 mm/s, P<0.01; n = 10; Figure 3). Morusin treatment reduced the number of central zone crossings, time spent in the central zone, total distance

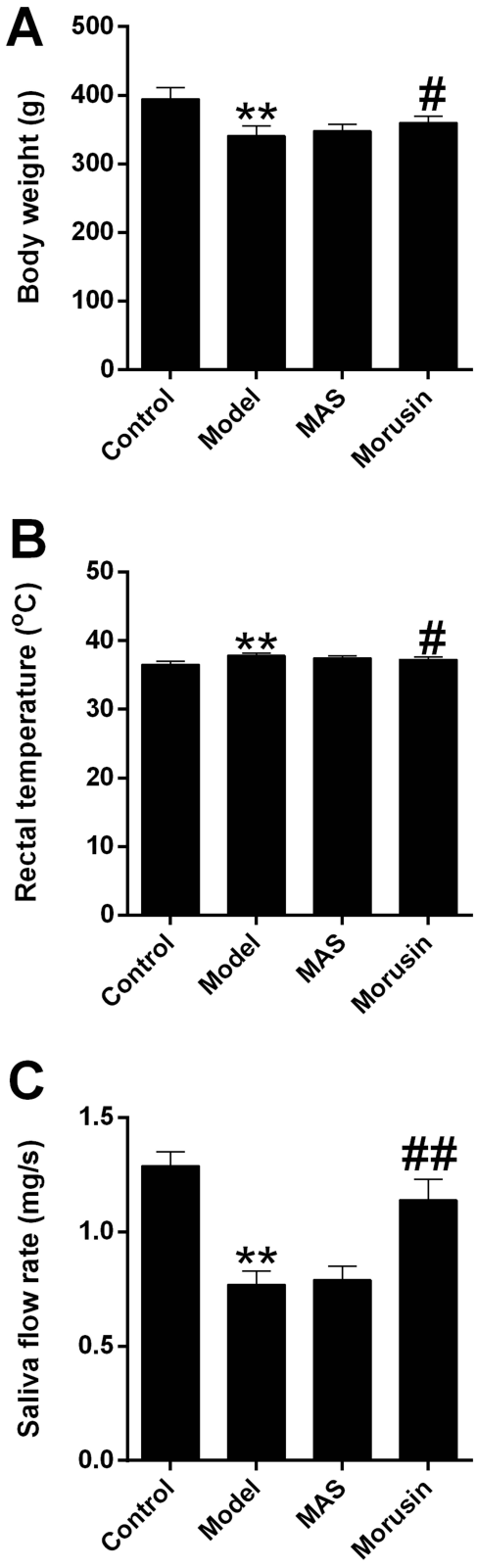

Figure 1 Effects of morusin and MAS on body weight, rectal temperature and saliva flow rate. The body weight (**A**), rectal temperature (**B**) and saliva flow rate (**C**) were evaluated in rats from different treatment groups. N = 10. $^{**}P<0.01$ compared to control group; $^{\#}P<0.05$ compared to Model group (One-way ANOVA followed by Bonferroni's multiple comparison tests).

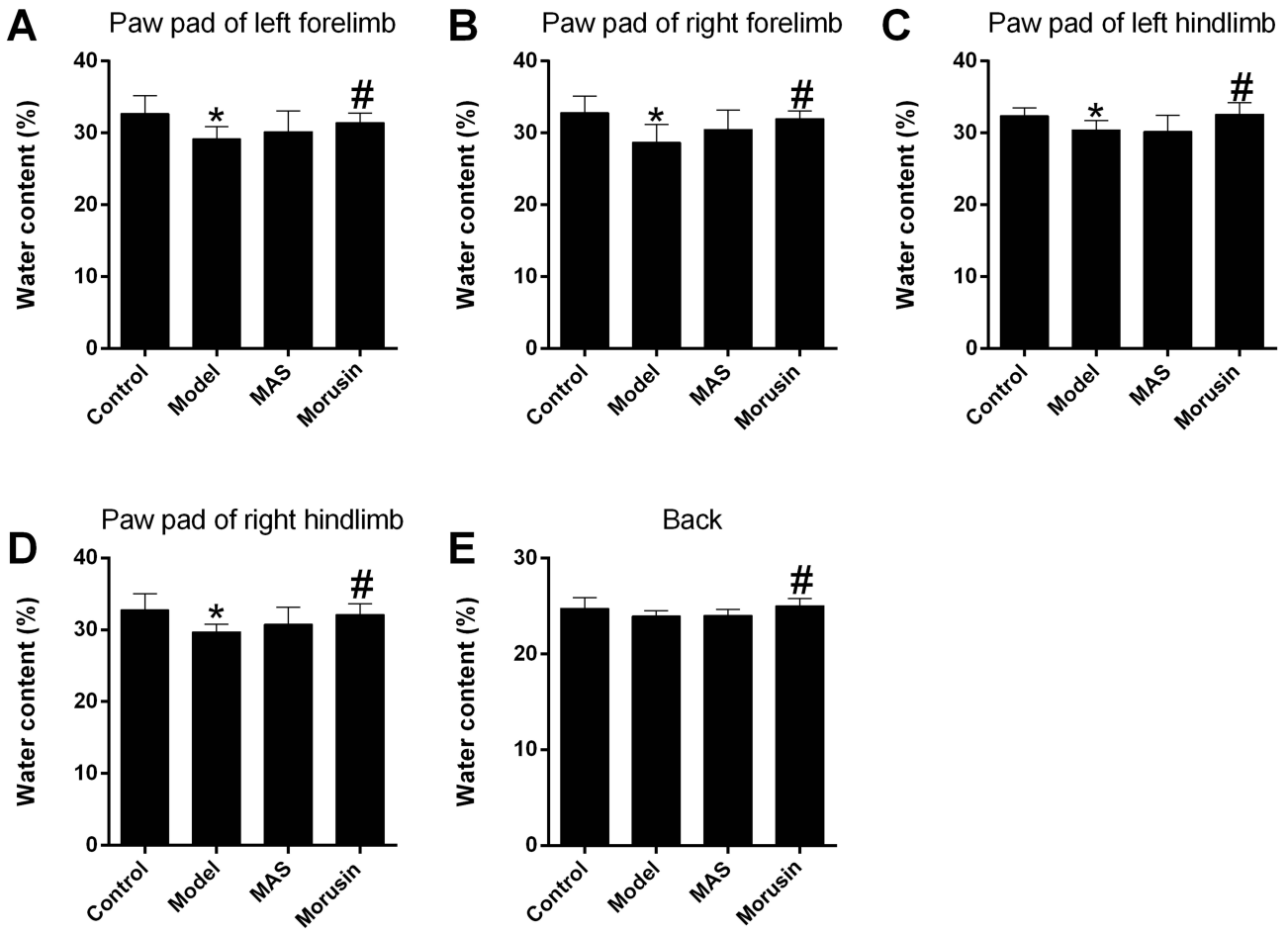

Figure 2 Effects of morusin and MAS on the water content in the rat skin. The water content in paw pad of left forelimb (**A**), paw pad of right forelimb (**B**), paw pad of left hindlimb (**C**), paw pad of right hindlimb (**D**) and the back (**E**) of rats from different treatment groups were evaluated. N = 10. *$P<0.05$ compared to control group; #$P<0.05$ compared to Model group (One-way ANOVA followed by Bonferroni's multiple comparison tests).

moved, and velocity compared to the model group (Number of central zone crossings: morusin group, 10.2 ± 1.8 versus model group, 14.2 ± 2.6, P<0.05; time spent in the central zone: morusin group, 21.4 ± 1.6% versus model group, 24.8 ± 2.3%, P<0.05; total distance moved: morusin group, 50.7 ± 3.4 m versus model group, 55.0 ± 2.7 m, P<0.05; velocity: morusin group, 18.0 ± 1.8 mm/s versus model group, 22.2 ± 3.7 mm/s, P<0.05; n = 10; Figure 3). MAS had no effect on the parameters of the open field test in the PIC model rats (Number of central zone crossings: MAS group, 13.5 ± 1.9 versus model group, 14.2 ± 2.6, P>0.05; time spent in the central zone: MAS group, 22.4 ± 1.5% versus model group, 24.8 ± 2.3%, P>0.05; total distance moved: MAS group, 51.7 ± 3.6 m versus model group, 55.0 ± 2.7 m, P>0.05; velocity: MAS group, 20.8 ± 2.1 mm/s versus model group, 22.2 ± 3.7 mm/s, P>0.05; n = 10; Figure 3).

Actions of Morusin and MAS on Airway Resistance of PIC Rats

Compared to the normal group, airway resistance increased under stimulation with acetylcholine at various concentrations in the model group (Table 1). Compared to the model group, rats in the morusin group showed a significant decrease in airway resistance under acetylcholine stimulation at various concentrations (except for 50 mg/mL) (Table 1). The MAS group also showed a decrease in airway resistance under acetylcholine stimulation at various concentrations in PIC rats (Table 1).

https://doi.org/10.2147/JIR.S550219

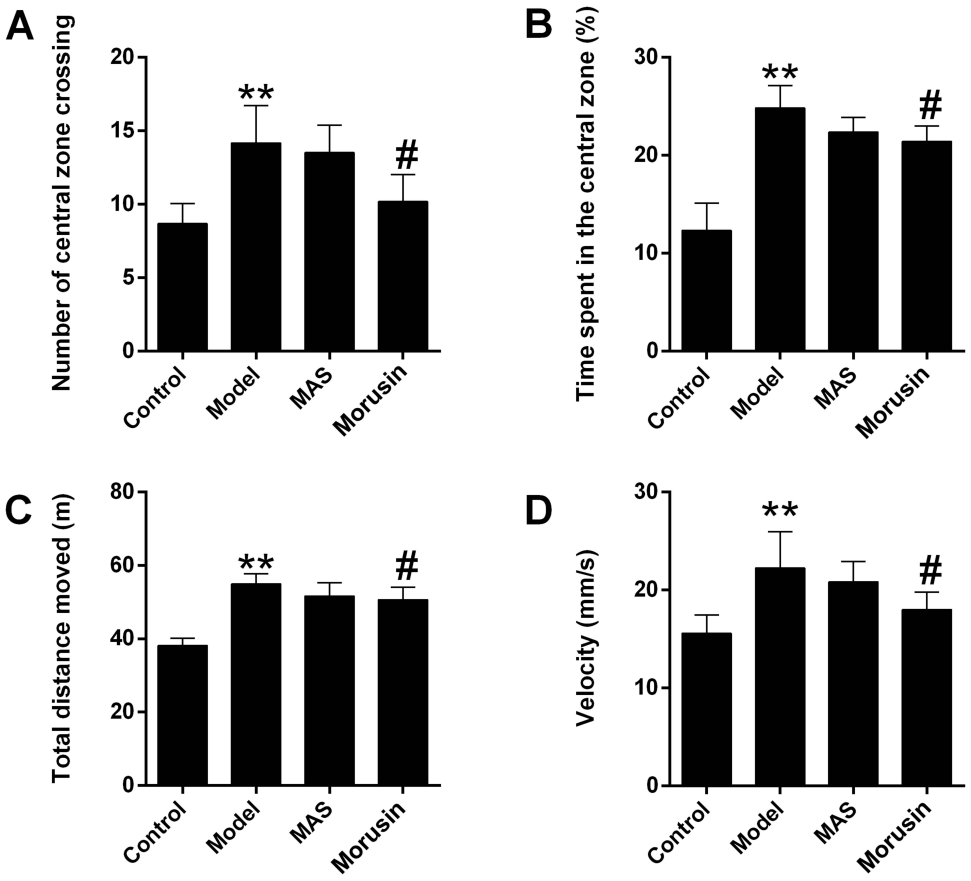

Figure 3 Effects of morusin and MAS on the parameters of open field test in rats. Number of central zone crossing (**A**), time spent in the central zone (%) (**B**), total distance moved (m) (**C**), and (**D**) velocity (mm/s) from different treatment groups were evaluated. N = 10. $^{**}P<0.01$ compared to control group; $^{\#}P<0.05$ compared to Model group (One-way ANOVA followed by Bonferroni's multiple comparison tests).

Effects of Morusin and MAS on Number of Airway Goblet Cells

In the normal group of rats, goblet cells are occasionally found in the airway epithelium, and mucus in the airway is minimal. In comparison, PIC model rats exhibited an increase in goblet cells in the airway mucosal epithelium, increased mucus secretion, and the presence of mucus plugs in the lumen compared to the control group (Figure 4). The percentage of goblet cells in the airway epithelium was higher in the model group than in the normal group (Model group, 9.3 ± 2.7 versus control group, 5.3 ± 1.0, P<0.05; n = 10; Figure 4). Rats from the morusin and MAS groups showed a decrease in goblet cell hyperplasia, reduced mucus secretion, and fewer mucus plugs in the lumen compared to the model group (Figure 4). The percentage of goblet cells in the airway of rats in the morusin and MAS groups was lower than in the model group (Morusin group, 6.0 ± 1.8 versus model group, 9.3 ± 2.7, P<0.05; MAS group, 6.8 ± 1.5 versus model group, 9.3 ± 2.7, P<0.05; n =10; Figure 4).

Table 1 Effects of Morusin and MAS on the Airway Resistance of the PIC Model Rats

Group	Acetylcholine (mg/mL)				
	0	6.25	12.5	25	50
Control (n=10)	0.37±0.05	0.46±0.04	0.63±0.04	0.78±0.05	0.81±0.31
Model (n=10)	0.46±0.04*	0.57±0.04**	0.69±0.03*	0.87±0.04*	0.95±0.10*
MAS (n=10)	$0.39\pm0.02^{\#\#}$	$0.50\pm0.03^{\#}$	$0.61\pm0.03^{\#\#}$	$0.81\pm0.02^{\#}$	$0.84\pm0.03^{\#}$
Morusin (n=10)	$0.41\pm0.03^{\#}$	$0.54\pm0.03^{\#}$	$0.63\pm0.04^{\#}$	$0.81\pm0.03^{\#}$	0.89±0.06

Notes: $^{*}P<0.05$ and $^{**}P<0.01$ compared to control group; $^{\#}P<0.05$ and $^{\#\#}P<0.01$ compared to Model group.
Abbreviations: MAS, montelukast sodium; PIC, post-infectious cough.

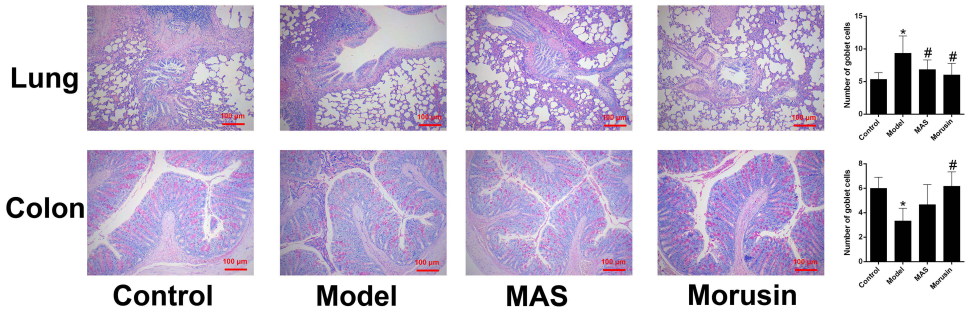

Figure 4 Effects of morusin and MAS on goblet cell number in lung and colon tissues. Goblet cells were evaluated with PAS staining in lung and colon tissues. N = 10. *P<0.05 compared to control group; #P<0.05 compared to Model group (One-way ANOVA followed by Bonferroni's multiple comparison tests).

Effects of Morusin and MAS on Colonic Goblet Cell Number

In colon tissues, goblet cells are located between the colonic mucosal epithelium and intestinal glandular epithelium, resembling goblets. These cells stain deep purple-red with PAS staining, and granular substances can be observed within them (Figure 4). There was a decrease in the number of goblet cells in rats from the model group compared to the control group (Model group, 3.3 ± 1.0 versus control group, 6.0 ± 0.9, P<0.05; n = 10; Figure 4). Compared to the model group, rats in the morusin group showed an increase in stained material within colonic goblet cells, more granules, and a higher number of goblet cells (Morusin group, 6.2 ± 1.2 versus model group, 3.3 ± 1.0, P<0.05; n = 10; Figure 4). MAS treatment had no effect on the number of colonic goblet cells in PIC model rats (MAS group, 4.7 ± 1.6 versus model group, 3.3 ± 1.0, P<0.05; n = 10; Figure 4).

Actions of Morusin and MAS on Expression of IL-4, −6 and −10 Protein

As shown in Figure 2, IL-4, IL-6, and IL-10 protein expressions were significantly upregulated in lung tissues from the model group compared to the control group (IL-4: model group, 0.088 ± 0.021 versus control group, 0.045 ± 0.004, P<0.05; IL-6: model group, 0.053 ± 0.009 versus control group, 0.025 ± 0.009, P<0.05; IL-10: model group, 0.013 ± 0.001 versus control group, 0.024 ± 0.005, P<0.05; n =10; Figure 5). Both morusin and MAS treatments significantly reduced IL-4, IL-6, and IL-10 protein levels in PIC model rats (IL-4: morusin group, 0.043 ± 0.004 versus model group, 0.088 ± 0.021, P<0.05; IL-6: morusin group, 0.026 ± 0.007 versus model group, 0.053 ± 0.009, P<0.05; IL-10: morusin group, 0.027 ± 0.003 versus model group, 0.013 ± 0.001, P<0.05; IL-4: MAS group, 0.046 ± 0.015 versus model group, 0.088 ± 0.021, P<0.05; IL-6: MAS group, 0.030 ± 0.007 versus model group, 0.053 ± 0.009, P<0.05; IL-10: MAS group, 0.025 ± 0.005 versus model group, 0.013 ± 0.001, P<0.05; n = 10; Figure 5).

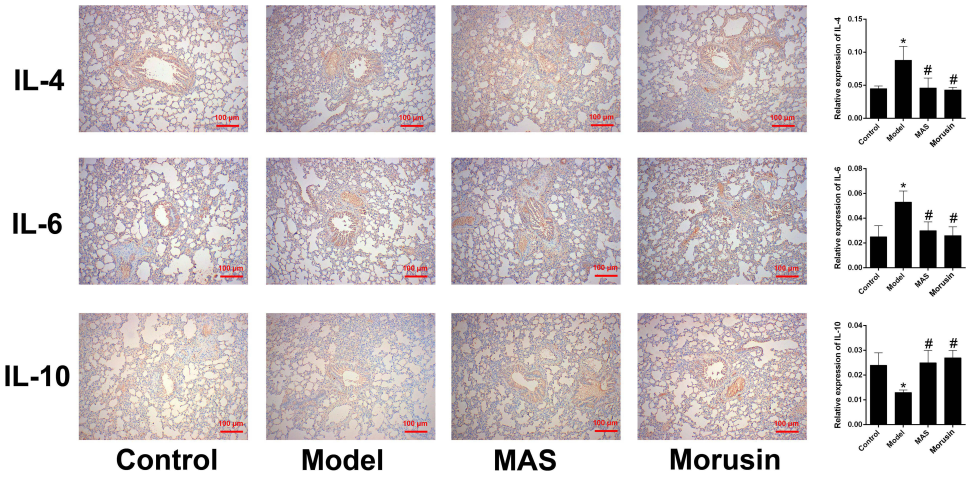

Figure 5 Effects of morusin and MAS on IL-4, −6 and 10 protein expression in lung tissues. IL-4, −6 and 10 proteins in lung tissues were detected immunostaining. N = 10. *P<0.05 compared to control group; #P<0.05 compared to Model group (One-way ANOVA followed by Bonferroni's multiple comparison tests).

https://doi.org/10.2147/JIR.S550219

Actions of Morusin and MAS on p-ERK1/2 Expression

As shown in Figure 3, p-ERK1/2 expression was upregulated in the lung and colon tissues of the model group compared to the control group (Lung: model group, 0.050 ± 0.006 versus control group, 0.021 ± 0.004, P<0.01; Colon: model group, 0.042 ± 0.005 versus control group, 0.019 ± 0.007, P<0.01; n =10; Figure 6). Morusin treatment reduced p-ERK1/2 expression in both lung and colon tissues of the model group (Lung: morusin group, 0.021 ± 0.003 versus model group, 0.050 ± 0.006, P<0.01; Colon: morusin group, 0.022 ± 0.004 versus model group, 0.042 ± 0.005, P<0.01; n = 10; Figure 6). MAS treatment only downregulated p-ERK1/2 expression in lung tissues, with no effect on colonic tissues in PIC model rats (Lung: MAS group, 0.023 ± 0.003 versus model group, 0.050 ± 0.006, P<0.01; Colon: MAS group, 0.030 ± 0.007 versus model group, 0.042 ± 0.005, P>0.05; n = 10; Figure 6).

Actions of Morusin and MAS on Rat Intestinal Microbiota

The Kruskal–Wallis rank-sum test was used to analyze differences in the taxonomic levels of intestinal microbiota among various rat groups. Results from multiple comparisons revealed significant differences among groups for genera such as Lactobacillus, Ruminococcus, Eubacterium_xylanophilum_group, unclassified_f_Lachnospiraceae, Lachnospiraceae_NK4A136_group, Akkermansia, and Treponema (Figure 7).

Pairwise comparisons showed that compared to the normal group, the abundance of the genus Lactobacillus was decreased in the model group (Lactobacillus: model group, 0.15 versus control group, 0.47, P<0.05; n = 10; Figure 8). However, compared to the model group, Lactobacillus abundance was significantly increased in the morusin group (Lactobacillus: morusin group, 0.56 versus model group, 0.15, P<0.05; n = 10; Figure 8). The abundance of genera Ruminococcus, Eubacterium_xylanophilum_group, unclassified_f_Lachnospiraceae, and Lachnospiraceae_NK4A136_group was increased in the model group compared to the normal group (Ruminococcus: model group, 0.033 versus control group, 0.0069, P<0.05; Eubacterium_xylanophilum_group: model group, 0.017 versus control group, 0.0021, P<0.05; unclassified_f_Lachnospiraceae: model group, 0.073 versus control group, 0.007, P<0.05; Lachnospiraceae_NK4A136_group: model group, 0.081 versus control group, 0.019, P<0.05; n = 10; Figure 8). Compared to the model group, the abundance of Ruminococcus, Eubacterium_xylanophilum_group, and Lachnospiraceae_NK4A136_group was decreased in the morusin group (Ruminococcus: Morusin group, 0.0021 versus model group, 0.033, P<0.05; Eubacterium_xylanophilum_group: Morusin group, 0.002 versus model group, 0.017, P<0.05; Lachnospiraceae_NK4A136_group: Morusin group, 0.001 versus model group, 0.081, P<0.05; n = 10; Figure 8), while the abundance of unclassified_f_Lachnospiraceae remained unaffected (unclassified_f_Lachnospiraceae: Morusin group, 0.018 versus model group, 0.073, P<0.05; n = 10; Figure 8). No significant changes were observed in the MAS group compared to the model group (Lactobacillus: MAS group, 0.22 versus control group, 0.15, P>0.05; Ruminococcus: MAS group, 0.028 versus control group, 0.033, P>0.05; Eubacterium_xylanophilum_group: MAS group, 0.017 versus control group, 0.017, P>0.05; unclassified_f_Lachnospiraceae: MAS group, 0.032 versus control group, 0.073, P>0.05; Lachnospiraceae_NK4A136_group: MAS group, 0.062 versus control group, 0.081, P>0.05; n = 10; Figure 8).

Additionally, the species with significant differences in abundance across the intestinal microbiota of each rat group are as follows: in the normal group, Lactobacillus and Allobaculum; in the model group, Lachnospiraceae_NK4A136_group,

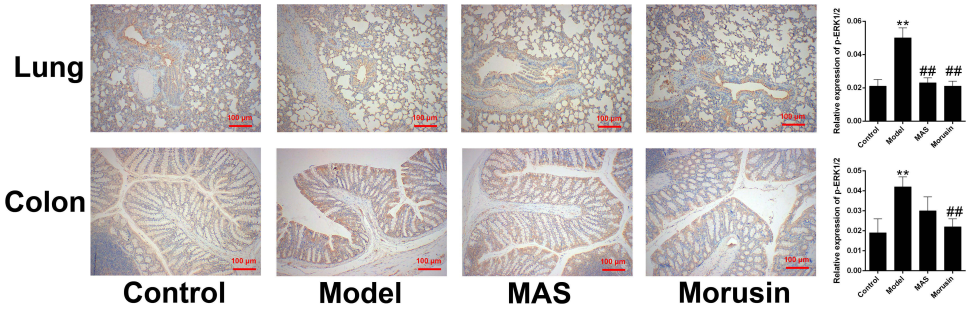

Figure 6 Effects of morusin and MAS on p-ERK protein expression in lung and colon tissues. P-ERK protein in lung and colon tissues were detected immunostaining. N = 10. $^{**}P<0.01$ compared to control group; $^{\#\#}P<0.01$ compared to Model group (One-way ANOVA followed by Bonferroni's multiple comparison tests).

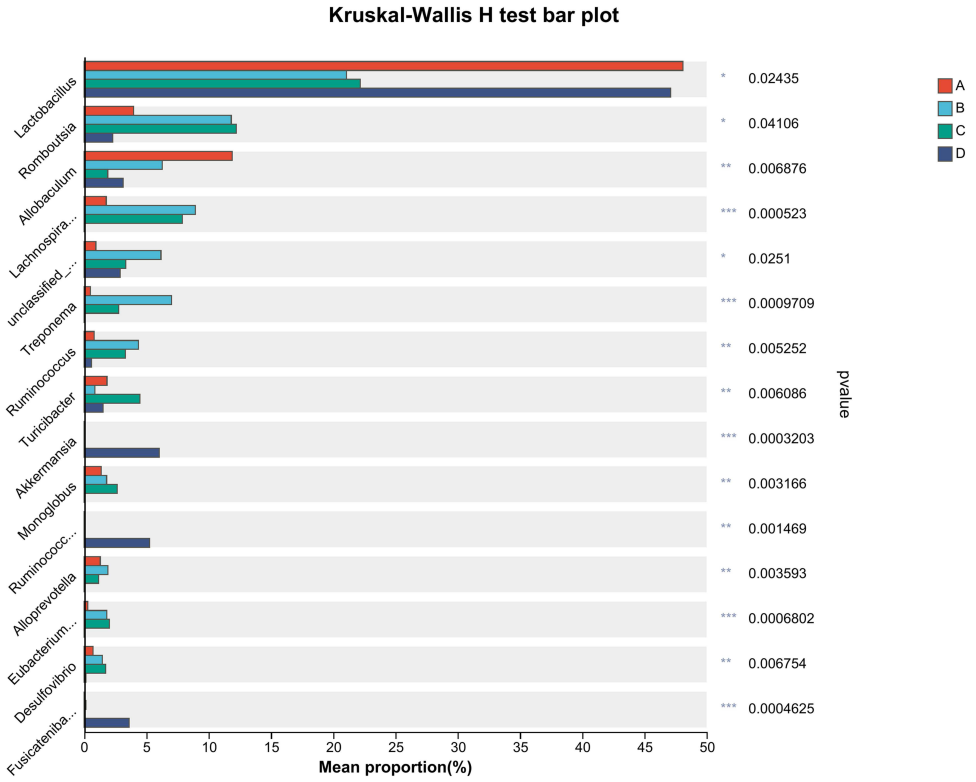

Figure 7 Comparative analysis of the relative abundance of different species in the gut microbiota of rats across multiple groups. (A) control group; (B) model group; (C) MAS group; (D) Morusin group. *P<0.05, **P<0.01 and ***P<0.001 (Kruskal–Wallis H-test).

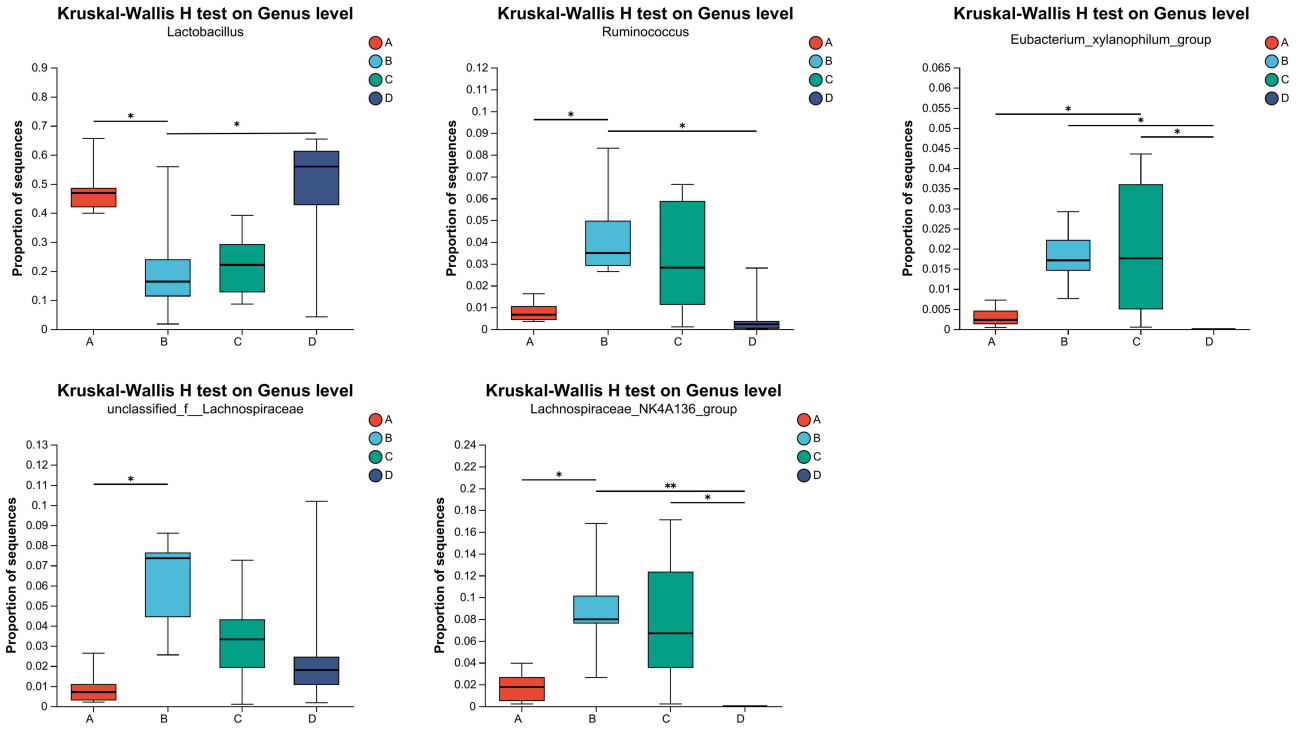

Figure 8 Inter-group comparison of the relative abundance of different species in the gut microbiota of rats. (**A**) control group; (**B**) model group; (**C**) MAS group; (**D**) Morusin group. *P<0.05 and **P<0.01 (Kruskal–Wallis H-test).

https://doi.org/10.2147/JIR.S550219

Treponema, unclassified_f_Lachnospiraceae, and Ruminococcus; in the MAS group, Romboutsia, Turicibacter, and Monoglobus; and in the morusin group, Fusicatenibacter, Ruminococcus_gnavus_group, Akkermansia, Blautia, and Bacteroides (Figure 9).

Correlation Analysis Between Rat Intestinal Microbiota and Various Factors

Figure 7 depicts the correlation between the intestinal microbiota of the four rat groups and the protein expression levels of IL-4, IL-6, and IL-10 in lung tissues at the genus level. Results demonstrated a positive correlation between IL-10 and Akkermansia, a dominant genus in the rat intestinal tract of the morusin group (P<0.01; Figure 10A). IL-10 showed negative correlations with Ruminococcus (P<0.05), Treponema (P<0.05), Lachnospiraceae_NK4A136_group (P<0.05), unclassified_f_Lachnospiraceae (P<0.05; Figure 10A). These genera, which are dominant in the rat intestinal tract of the model group with significantly increased abundance, can be reduced by morusin.

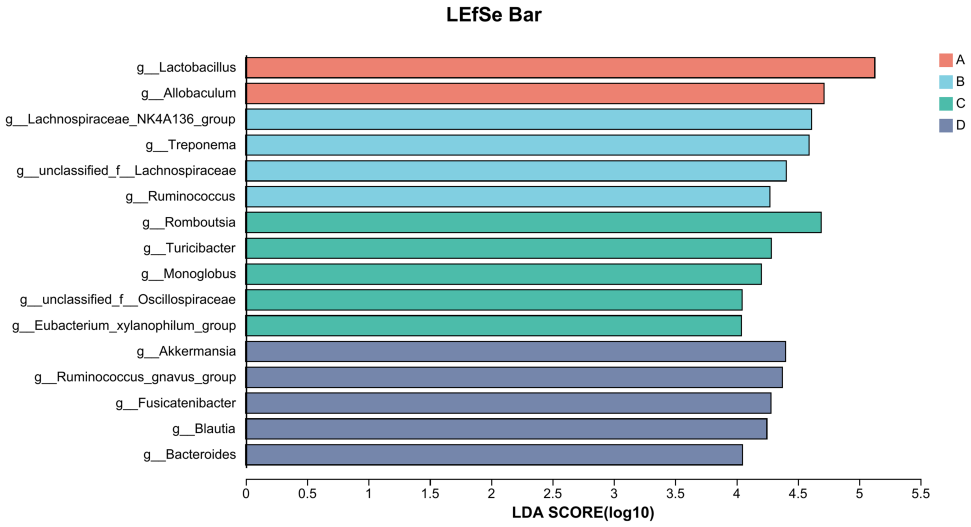

Figure 9 LEfSe comparison of the gut microbiota among different treatment groups. The length of the bar represents the LDA score. (**A**) control group; (**B**) model group; (**C**) MAS group; (**D**) Morusin group.

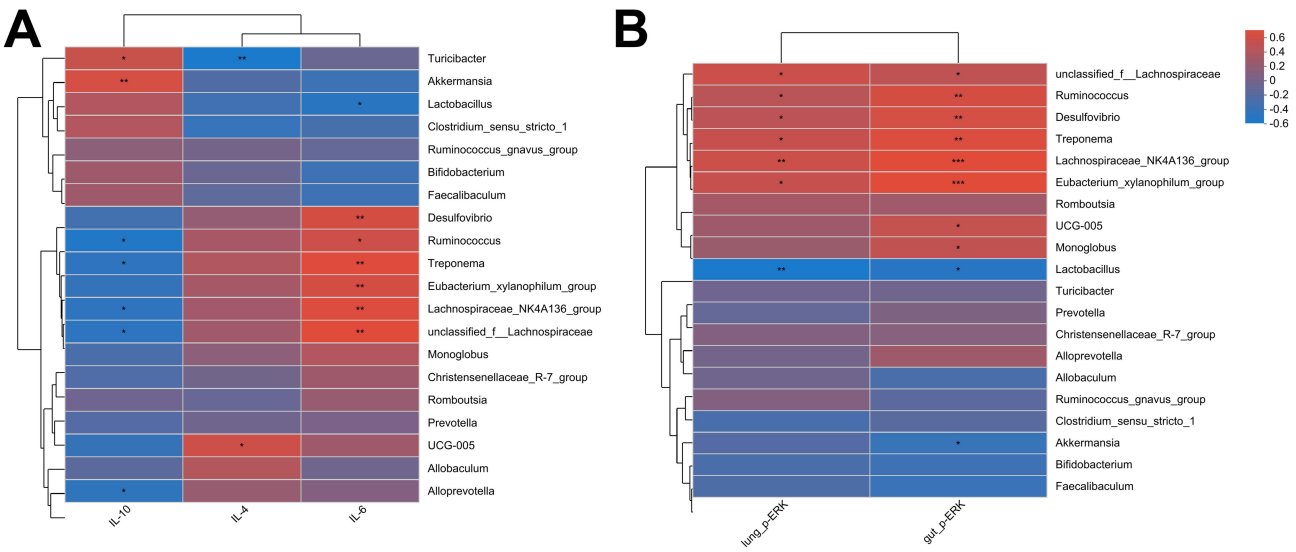

Figure 10 Pearson's correlation heat map analysis of bacterial abundance and environmental factors (IL-4, 6, 10, p-ERK levels). (**A**) Correlation between bacterial abundance and IL-4/-6/-10 in lung tissues. (**B**) Correlation between bacterial abundance and p-ERK in lung/colon tissues. Red represents a positive correlation and blue represents a negative correlation. *P < 0.05, **P<0.01 and ***P < 0.001.

IL-6 exhibited a negative correlation with Lactobacillus (P<0.05; Figure 10A), a dominant genus in the rat intestinal tract of the normal group, with decreased abundance in the model group, which can be adjusted by morusin (Figure 10A). IL-6 showed positive correlations with Ruminococcus (P<0.05), Treponema (P<0.01), Eubacterium_xylanophilum_group (P<0.01), Lachnospiraceae_NK4A136_group (P<0.01), and unclassified_f_Lachnospiraceae (P<0.01; Figure 10A), all of which are dominant genera in the intestinal tract of rats in the model group, with significantly increased abundance, which can be decreased by morusin. IL-4 exhibited a negative association with Turicibacter (P<0.01) and a positive association with UCG-005 (P<0.05; Figure 10A).

A correlation heatmap was generated to illustrate the relationship between the intestinal microbiota of the four rat groups and p-ERK protein expression in lung and colon tissues at the genus level. Results showed a positive correlation between p-ERK protein and genera such as Lachnospiraceae_NK4A136_group (P<0.01), unclassified_f_Lachnospiraceae (P<0.05), Ruminococcus (P<0.05), Eubacterium_xylanophilum_group (P<0.05), and Treponema (P<0.05; Figure 10B). These genera are dominant in the rat intestinal tract of the model group, with significantly increased abundance, which can be reduced by morusin.There was a negative correlation between p-ERK protein expression and the genus Lactobacillus (Figure 10B). Additionally, in colon tissue, p-ERK protein showed a negative correlation with Akkermansia (P<0.05; Figure 10B). Lactobacillus is a dominant genus in the rat intestinal tract of the normal group, while Akkermansia is a dominant genus in the morusin group (Figure 10B).

Discussion

In the "Clinical Practice Guidelines for Diagnosis and Treatment of Pediatric Cough in China (2021 Edition)",[1] it is noted that PIC is a common cause of chronic cough in children. This persistent and unresolved cough severely affects the quality of life of affected children and can be detrimental to their growth and development. PIC is believed to result from damage to the respiratory epithelium caused by respiratory pathogen infection.[22] This disruption of respiratory function leads to hyperreactivity and airway inflammation, which together increase cough sensitivity, ultimately resulting in a persistent and unresolved cough.[23] Therefore, alleviating airway inflammation and reducing airway hyperreactivity are key to PIC treatment. In comparison to our previous work,[24] this study uniquely investigates the modulatory effects of morusin on the ERK signaling pathway in both lung and colon tissues, along with detailed correlation analysis between specific cytokines (IL-4, IL-6, IL-10) and gut microbiota genera. The comprehensive assessment includes a broad range of physiological metrics and reveals novel findings on goblet cell numbers in both lung and colon tissues, showcasing morusin 's systemic effects. These insights into morusin's regulation of gut microbiota composition and its role in immune modulation and airway inflammation reduction provide new therapeutic avenues for managing PIC.

The open field test is chosen for investigating animal behavior in a PIC model due to its ability to assess general locomotor activity, anxiety-like behavior, and exploratory behavior in rodents.[25,26] This test is crucial for understanding if infections or resulting coughs affect these behaviors, indicating broader neurological or physiological impacts.[25,26] It helps monitor changes in physical activity, assess stress and anxiety levels induced by respiratory issues, and provides a non-invasive, simple, and repeatable method for tracking behavioral changes over time.[27] In our study, rats from the model group showed significant increases in the number of central zone crossings, time spent in the central zone, total distance moved, and velocity compared to the control group. Treatment with morusin reduced these parameters in the model group. However, MAS treatment did not affect any of these parameters in the PIC model rats. Our findings indicate that PIC significantly affects locomotor activity and anxiety-like behavior in rats. Morusin treatment appears effective in mitigating these effects, while MAS does not. These results contribute to understanding the broader impacts of respiratory infections and the potential benefits of specific treatments in addressing related behavioral changes.

Increasing evidence reveals that modulation in gut microbiota diversity was related to airway inflammation and hyperreactivity.[28] This process involves signaling pathways.[29,30] Thus, modulating the gut microbiota to inhibit relevant signaling pathways and alleviate airway inflammation and hyperreactivity may become potential targets for PIC treatment.[29]

The "lung-gut axis" concept within modern medicine has imbued the theories of the "reciprocal relationship between the lungs and large intestine" and "lung-intestine combined treatment" with scientific underpinnings.[31,32] Studies have demonstrated that various factors such as hypoxia, inflammatory responses, and prolonged antibiotic use, typical in pulmonary diseases, can compromise intestinal mucosal barrier integrity, disrupt gut microbiota balance, or trigger the

release of endotoxins.[33] Additionally, dysbiosis of the gut microbiota has emerged as a novel pathogenic element influencing the progression of pulmonary diseases. It is evident that microbes may act as mediators between the lungs and the large intestine, potentially involving relevant signaling pathways.

For instance, changes in gut microbiota diversity can affect the intestinal environment and its metabolites, stimulating the expression of GPR41/GPR43 receptors on immune cell surfaces and activating signaling pathways such as ERK1/2 by modulating inositol triphosphate (IP3) levels and cyclic adenosine monophosphate (cAMP) content. This modulation impacts the proliferation of inflammatory T lymphocytes, as well as the production of inflammatory cytokines (including IL-4 and IL-6) and the anti-inflammatory factor IL-10.[34,35] These substances are closely associated with airway inflammation and hyperreactivity, which are key pathogenic mechanisms underlying PIC. Thus, the gut microbiota's influence on ERK signaling appears pivotal in PIC progression.

Our results showed that compared to the normal group, p-ERK1/2 protein expression in the lung and colon tissues of model rats was elevated, indicating activation of ERK signaling. Morusin reduced p-ERK1/2 protein expression in these tissues, thereby inhibiting ERK signaling. Analysis of gut microbiota revealed that the inflammatory factor IL-6 and p-ERK protein expression in lung and colon tissues were negatively correlated with the genus Lactobacillus. Lactobacillus is the dominant genus in the intestinal tract of normal rats, and its abundance significantly decreases in the model group. Morusin effectively restored Lactobacillus abundance; studies have shown that Lactobacillus can degrade pro-inflammatory chemokines, exert anti-inflammatory effects, and inhibit airway inflammation and remodeling in mice.[36] Furthermore, the expression of the anti-inflammatory factor IL-10 was positively correlated with the genus Akkermansia, while p-ERK protein expression in colon tissues was negatively correlated with Akkermansia. Akkermansia is the dominant genus in the intestinal tract of rats in the lung-intestine combined treatment group. It is a newly discovered beneficial gut microorganism that regulates intestinal barrier function and is negatively correlated with inflammation and metabolic disorders. Akkermansia can activate host immune responses to combat respiratory inflammation and maintain lung health.[37]

Our findings in the PIC model extend the growing body of evidence that morusin exerts broad anti-inflammatory and barrier-protective effects across diverse tissues and disease contexts. In chondrocytes and osteoarthritic joints, Jia et al demonstrated that morusin suppresses IL-1β–induced TNF-α, IL-6, iNOS, COX2, ADAMTS5, and MMP expression by inhibiting p65 phosphorylation and IκBα degradation via the NF-κB pathway, both in vitro and in a destabilization-of-the-medial-meniscus model in mice.[6] Similarly, our study shows that morusin reduces lung IL-4, IL-6, and IL-10 levels and downregulates p-ERK1/2 in lung and colon tissues, accompanied by restoration of body weight, salivary secretion, skin hydration, and normalization of open-field behavior. These parallels suggest that NF-κB inhibition—and perhaps intersecting MAPK/ERK modulation—underlies morusin's systemic efficacy in PIC, echoing its chondroprotective mechanism.

Beyond NF-κB, morusin has been shown to engage additional signaling axes to fortify epithelial barriers and mitigate fibrosis. In ruminal epithelial cells, Yang et al reported that morusin attenuates LPS-triggered inflammation by blocking EGFR-driven AKT and NF-κB p65 phosphorylation and enhancing barrier-function genes,[7] while Kang et al uncovered in diabetic mice that morusin activates SIRT1 to destabilize HIF-1α, thereby reducing IL-16, ECM accumulation, and tubular apoptosis.[38] Concordant with these multifactorial modes, we observed morusin, specific remodeling of the gut microbiota, boosting Lactobacillus and Akkermansia, suppressing Ruminococcus and Lachnospiraceae groups—which correlates inversely with IL-6, IL-10, and p-ERK1/2 expression. This microbiota–immune crosstalk may represent an additional dimension of morusin's action, bridging its epithelial-barrier and anti-fibrotic properties to systemic immune regulation in PIC.

Our work advances the PIC field beyond recent lung–gut axis studies in several ways. First, we provide a direct head-to-head comparison showing that, unlike MAS, morusin exerts dual-site suppression of ERK signaling in both lung and colon while simultaneously remodeling the gut microbiota. This remodeling enriches beneficial genera (Lactobacillus, Akkermansia) and reduces pro-inflammatory taxa, thereby linking immune modulation with ERK control across the gut–lung axis. Second, we integrate systemic (body weight, salivary flow, skin hydration), behavioral (open-field), airway (resistance, goblet cell hyperplasia), and molecular (tissue ERK signaling) readouts, offering a multi-scale dataset rarely reported in respiratory or probiotic-focused studies. Third, we delineate a microbiota–immune–ERK axis by correlating microbial shifts with cytokine profiles (positive association of Akkermansia with IL-10; negative association of Lactobacillus with IL-6) and with p-ERK levels in lung and colon. These findings extend earlier reports by identifying

ERK as a tractable downstream node in PIC pathogenesis. Importantly, whereas prior studies generally noted correlations between beneficial microbiota and anti-inflammatory cytokines, our data uniquely demonstrate that morusin, unlike MAS, coordinates microbiota remodeling, colon ERK suppression, and behavioral rescue, underscoring its broader and mechanistically integrated efficacy. Collectively, these distinctions highlight morusin's translational promise as a candidate that addresses both airway pathology and the upstream microbial–immune drivers of PIC.

Although both morusin and MAS attenuated airway inflammation, only morusin normalized anxiety-like hyperactivity and locomotor activity in the open-field test. This discrepancy may reflect differences in pharmacological mechanisms and systemic actions: MAS primarily antagonizes cysteinyl leukotriene receptors[39] and reduced p-ERK1/2 expression only in lung tissue, without affecting colonic ERK signaling or remodeling the gut microbiota, thereby limiting its influence on the gut–lung–brain axis that contributes to behavioral outcomes. In contrast, morusin exerted broader effects, simultaneously suppressing ERK activity in both lung and colon tissues, rebalancing key microbiota genera (Lactobacillus, Akkermansia), and restoring systemic parameters such as body weight, salivary secretion, and skin hydration, providing a mechanistic basis for behavioral improvement. Additionally, the MAS dosing regimen may have been sufficient for airway resistance but inadequate to induce systemic or behavioral benefits, and our sample size, powered for airway outcomes rather than behavior, may have limited the detection of smaller effects. Taken together, these findings highlight the biological significance of morusin's multifaceted actions and suggest that MAS's lack of behavioral efficacy may stem from its narrower pharmacological profile and treatment exposure.

This study has several limitations: it relied solely on a male-only PIC rat model, which may not fully recapitulate human immune–microbiota interactions or sex-specific responses; only a single dosing regimen of morusin and MAS was tested without pharmacokinetic or dose–response data to confirm optimal exposure; mechanistic links between microbiota shifts and cytokine or p-ERK1/2 suppression remain correlative, lacking causal validation via functional assays; microbiota profiling was limited to 16S rRNA genus-level resolution without deeper metagenomic or metabolomic analyses to pinpoint active species or metabolites; and all outcomes were assessed shortly after treatment, leaving the durability, long-term safety, and potential tolerance to morusin uncharacterized. In addition, future research should expand to include female models, long-term interventions, and humanized animal systems that better reflect clinical conditions, thereby enhancing translational relevance.

Conclusions

Morusin markedly alleviates PIC-induced systemic and mucosal dysfunction by restoring body weight, salivary secretion, skin hydration, and normalizing behavioral hyperactivity, while MAS shows no such benefits. At the tissue level, morusin reduces airway resistance, goblet cell hyperplasia in lung and colon, and suppresses IL-4, IL-6, IL-10, and p-ERK1/2 overexpression, whereas MAS only modestly affects airway resistance and lung p-ERK1/2. Importantly, morusin uniquely rebalances the gut microbiota—enhancing beneficial Lactobacillus and Akkermansia and suppressing pro-inflammatory taxa—with these shifts correlating inversely with cytokine and p-ERK1/2 levels, implicating a microbiota–immune axis in its multifaceted therapeutic action. These findings suggest that morusin may represent a promising candidate for developing novel therapies to manage post-infectious cough, offering translational potential for pediatric respiratory care where effective treatments are currently limited.

Data Sharing Statement

Data will be made available on request.

Ethics Statement

All the animal experiments were approved by the Animal Ethics Committee of Shenzhen Qianhai Shekou Free Trade Zone Hospital (No.20210110). The experiments were conducted in strict compliance with the National Laboratory Animal Welfare Standards: Laboratory Animal—Guideline for Ethical Review of Animal Welfare (GB/T35892–2018).

Author Contributions

JL and YD designed the whole study; JL, DZ and MZ performed the experiments; MZ and YC performed the data analysis and prepared the figures; JL and YD drafted the manuscript; all the authors approved the manuscript for submission.

Funding

This work was supported by Shenzhen Key Discipline Construction Funding Project of Traditional Chinese Medicine, Hunan Provincial Natural Science Foundation Project (No. 2023JJ60260), the Scientific Research Project of Guangdong Provincial Bureau of Traditional Chinese Medicine (No. 20241256), Shenzhen Fundamental Research Program (Natural Science Foundation) (JCYJ20240813153914019), and Major Science and Technology Project of the Health System in Nanshan District, Shenzhen (NSZD2024055).

Disclosure

The authors report no conflicts of interest in this work.

References

1. of Pharmacology SG, for Child NC, Board E. Clinical practice guidelines for the diagnosis and management of children with cough in China (version 2021). *Zhonghua Er Ke Za Zhi*. 2021;59(9):720–729. doi:10.3760/cma.j.cn112140-20210513-00423
2. Jiang W, Qi J, Li X, et al. Post-infectious cough of different syndromes treated by traditional Chinese medicines: a review. *Chin Herb Med*. 2022;14(4):494–510. doi:10.1016/j.chmed.2022.09.002
3. Choi DW, Cho SW, Lee SG, Choi CY. The beneficial effects of Morusin, an isoprene flavonoid isolated from the root bark of Morus. *Int J Mol Sci*. 2020;21(18). doi:10.3390/ijms21186541
4. Hafeez A, Khan Z, Armaghan M, et al. Exploring the therapeutic and anti-tumor properties of Morusin: a review of recent advances. *Front Mol Biosci*. 2023;10:1168298. doi:10.3389/fmolb.2023.1168298
5. Memete AR, Timar AV, Vuscan AN, Miere Groza F, Venter AC, Vicas SI. Phytochemical composition of different botanical parts of Morus species, health benefits and application in food industry. *Plants*. 2022;11(2). doi:10.3390/plants11020152
6. Jia Y, He W, Zhang H, et al. Morusin ameliorates il-1β-induced chondrocyte inflammation and osteoarthritis via NF-κB signal pathway. *Drug Des Devel Ther*. 2020;14:1227–1240. doi:10.2147/dddt.S244462
7. Yang C, Deng X, Wu L, Jiang T, Fu Z, Li J. Morusin protected ruminal epithelial cells against lipopolysaccharide-induced inflammation through inhibiting EGFR-AKT/NF-κB signaling and improving barrier functions. *Int J Mol Sci*. 2022;23(22):14428. doi:10.3390/ijms232214428
8. Zheng D, Liwinski T, Elinav E. Interaction between microbiota and immunity in health and disease. *Cell Res*. 2020;30(6):492–506. doi:10.1038/s41422-020-0332-7
9. Budden KF, Gellatly SL, Wood DL, et al. Emerging pathogenic links between microbiota and the gut-lung axis. *Nat Rev Microbiol*. 2017;15(1):55–63. doi:10.1038/nrmicro.2016.142
10. Li N, Dai Z, Wang Z, et al. Gut microbiota dysbiosis contributes to the development of chronic obstructive pulmonary disease. *Respir Res*. 2021;22(1):274. doi:10.1186/s12931-021-01872-z
11. Sriwastva MK, Deng ZB, Wang B, et al. Exosome-like nanoparticles from Mulberry bark prevent DSS-induced colitis via the AhR/COPS8 pathway. *EMBO Rep*. 2022;23(3):e53365. doi:10.15252/embr.202153365
12. Du Y, Zhang R, Zheng XX, et al. Mulberry (Morus alba L.) leaf water extract attenuates type 2 diabetes mellitus by regulating gut microbiota dysbiosis, lipopolysaccharide elevation and endocannabinoid system disorder. *J Ethnopharmacol*. 2024;323:117681. doi:10.1016/j.jep.2023.117681
13. Hu TG, Wen P, Fu HZ, Lin GY, Liao ST, Zou YX. Protective effect of mulberry (Morus atropurpurea) fruit against diphenoxylate-induced constipation in mice through the modulation of gut microbiota. *Food Funct*. 2019;10(3):1513–1528. doi:10.1039/c9fo00132h
14. Goplen N, Karim Z, Guo L, et al. ERK1 is important for Th2 differentiation and development of experimental asthma. *FASEB j*. 2012;26(5):1934–1945. doi:10.1096/fj.11-196477
15. Naqvi KF, Mazzone SB, Shiloh MU. Infectious and inflammatory pathways to cough. *Annu Rev Physiol*. 2023;85(1):71–91. doi:10.1146/annurev-physiol-031422-092315
16. Deng Z, Ding W, Li F, Shen S, Huang C, Lai K. Pulmonary IFN-γ causes lymphocytic inflammation and cough hypersensitivity by increasing the number of IFN-γ-secreting T lymphocytes. *Allergy Asthma Immunol Res*. 2022;14(6):653–673. doi:10.4168/aair.2022.14.6.653
17. Diard S, Liévin-Le Moal V, Toribio AL, et al. Norepinephrine-dependently released Dr fimbriae of diffusely adhering escherichia coli strain IH11128 promotes a mitogen-activated protein kinase ERK1/2-dependent production of pro-inflammatory cytokine, IL-8 in human intestinal Caco-2/TC7 cells. *Microb Infect*. 2009;11(10):886–894. doi:10.1016/j.micinf.2009.05.010
18. Li C, Chen W, Lin F, et al. Functional two-way crosstalk between brain and lung: the brain–lung axis. *Cell Mol Neurobiol*. 2023;43(3):991–1003. doi:10.1007/s10571-022-01238-z
19. Wang J, Liu X, Zheng H, et al. Morusin induces apoptosis and autophagy via JNK, ERK and PI3K/Akt signaling in human lung carcinoma cells. *Chem Biol Interact*. 2020;331:109279. doi:10.1016/j.cbi.2020.109279
20. Huang CC, Wang PH, Lu YT, et al. Morusin suppresses cancer cell invasion and MMP-2 expression through ERK signaling in human nasopharyngeal carcinoma. *Molecules*. 2020;25(20):4851. doi:10.3390/molecules25204851
21. Vochyánová Z, Pokorná M, Rotrekl D, et al. Prenylated flavonoid morusin protects against TNBS-induced colitis in rats. *PLoS One*. 2017;12(8):e0182464. doi:10.1371/journal.pone.0182464
22. Clementi N, Ghosh S, De Santis M, et al. Viral respiratory pathogens and lung injury. *Clin Microbiol Rev*. 2021;34(3). doi:10.1128/cmr.00103-20

23. Chung KF, McGarvey L, Song WJ, et al. Cough hypersensitivity and chronic cough. *Nat Rev Dis Primers*. 2022;8(1):45. doi:10.1038/s41572-022-00370-w
24. Luo J, Deng Y, Ding Y, et al. Investigation into actions of Xiebai and Zengye decoction on cough sensitivity, airway inflammation and gut microbiota in the rat model of post-infectious cough. *Heliyon*. 2023;9(12):e22782. doi:10.1016/j.heliyon.2023.e22782
25. Sarkar D, Sarkar D. A review of behavioral tests to evaluate different types of anxiety and anti-anxiety effects. *Clin Psychopharmacol Neurosci*. 2020;18(3):341–351. doi:10.9758/cpn.2020.18.3.341
26. Prut L, Belzung C. The open field as a paradigm to measure the effects of drugs on anxiety-like behaviors: a review. *Eur J Pharmacol*. 2003;463(1–3):3–33. doi:10.1016/s0014-2999(03)01272-x
27. Campos AC, Fogaça MV, Aguiar DC, Guimarães FS. Animal models of anxiety disorders and stress. *Braz J Psychiatry*. 2013;35(Suppl 2):S101–11. doi:10.1590/1516-4446-2013-1139
28. Wilson NG, Hernandez-Leyva A, Rosen AL, et al. The gut microbiota of people with asthma influences lung inflammation in gnotobiotic mice. *iScience*. 2023;26(2):105991. doi:10.1016/j.isci.2023.105991
29. Zhao X, Hu M, Zhou H, et al. The role of gut microbiome in the complex relationship between respiratory tract infection and asthma. *Front Microbiol*. 2023;14:1219942. doi:10.3389/fmicb.2023.1219942
30. Wang Z, Lai Z, Zhang X, et al. Altered gut microbiome compositions are associated with the severity of asthma. *J Thoracic Dis*. 2021;13(7):4322–4338. doi:10.21037/jtd-20-2189
31. Dang AT, Marsland BJ. Microbes, metabolites, and the gut-lung axis. *Mucosal Immunol*. 2019;12(4):843–850. doi:10.1038/s41385-019-0160-6
32. Saint-Criq V, Lugo-Villarino G, Thomas M. Dysbiosis, malnutrition and enhanced gut-lung axis contribute to age-related respiratory diseases. *Ageing Res Rev*. 2021;66:101235. doi:10.1016/j.arr.2020.101235
33. Zhu W, Wu Y, Liu H, Jiang C, Huo L. Gut-lung axis: microbial crosstalk in pediatric respiratory tract infections. *Front Immunol*. 2021;12:741233. doi:10.3389/fimmu.2021.741233
34. Osbelt L, Thiemann S, Smit N, et al. Variations in microbiota composition of laboratory mice influence citrobacter rodentium infection via variable short-chain fatty acid production. *PLoS Pathog*. 2020;16(3):e1008448. doi:10.1371/journal.ppat.1008448
35. Stark JM, Tibbitt CA, Coquet JM. The metabolic requirements of Th2 cell differentiation. *Front Immunol*. 2019;10:2318. doi:10.3389/fimmu.2019.02318
36. Hsieh MH, Jan RL, Wu LS, et al. Lactobacillus gasseri attenuates allergic airway inflammation through PPARγ activation in dendritic cells. *J Mol Med*. 2018;96(1):39–51. doi:10.1007/s00109-017-1598-1
37. Casaro MB, Thomas AM, Mendes E, et al. A probiotic has differential effects on allergic airway inflammation in A/J and C57BL/6 mice and is correlated with the gut microbiome. *Microbiome*. 2021;9(1):134. doi:10.1186/s40168-021-01081-2
38. Kang P, Xiao L, Liu Y, Yang J, Li S, Wang L. Morusin ameliorates tubulointerstitial damage in diabetic mice through SIRT1/HIF-1α/IL-16 signaling pathway. *Phytomedicine*. 2025;142:156781. doi:10.1016/j.phymed.2025.156781
39. Theron AJ, Steel HC, Tintinger GR, Gravett CM, Anderson R, Feldman C. Cysteinyl leukotriene receptor-1 antagonists as modulators of innate immune cell function. *J Immunol Res*. 2014;2014:608930. doi:10.1155/2014/608930

Journal of Inflammation Research

Dovepress
Taylor & Francis Group

Publish your work in this journal

The Journal of Inflammation Research is an international, peer-reviewed open-access journal that welcomes laboratory and clinical findings on the molecular basis, cell biology and pharmacology of inflammation including original research, reviews, symposium reports, hypothesis formation and commentaries on: acute/chronic inflammation; mediators of inflammation; cellular processes; molecular mechanisms; pharmacology and novel anti-inflammatory drugs; clinical conditions involving inflammation. The manuscript management system is completely online and includes a very quick and fair peer-review system. Visit http://www.dovepress.com/testimonials.php to read real quotes from published authors.

Submit your manuscript here: https://www.dovepress.com/journal-of-inflammation-research-journal